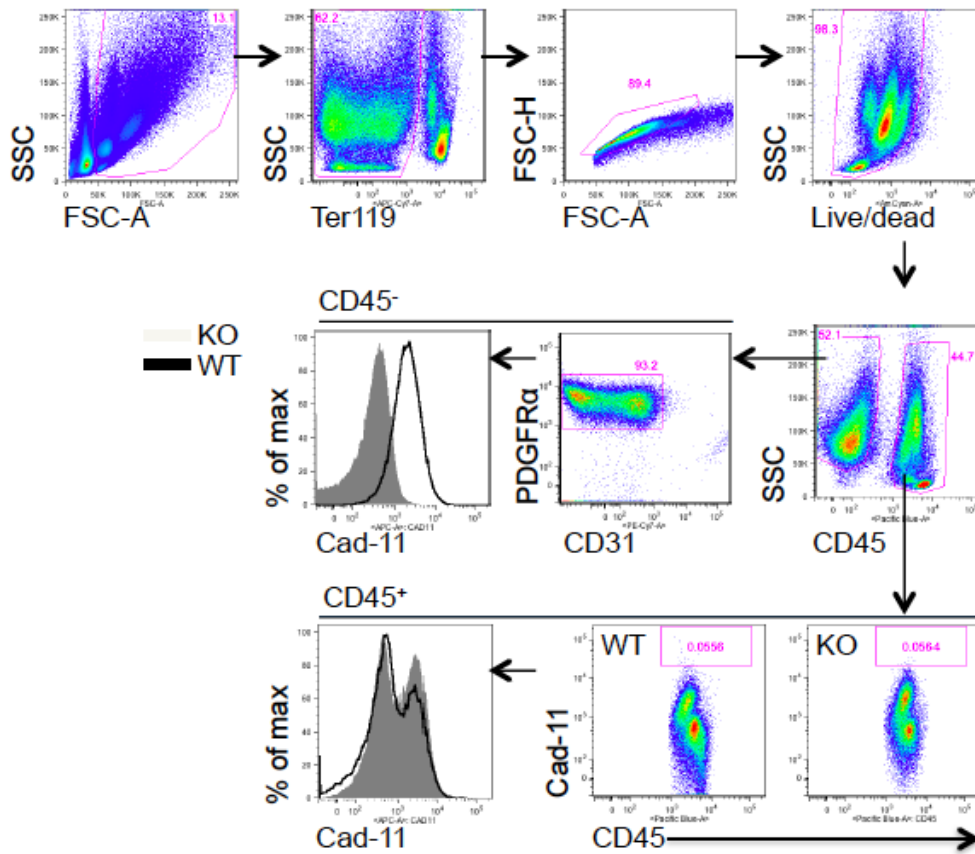


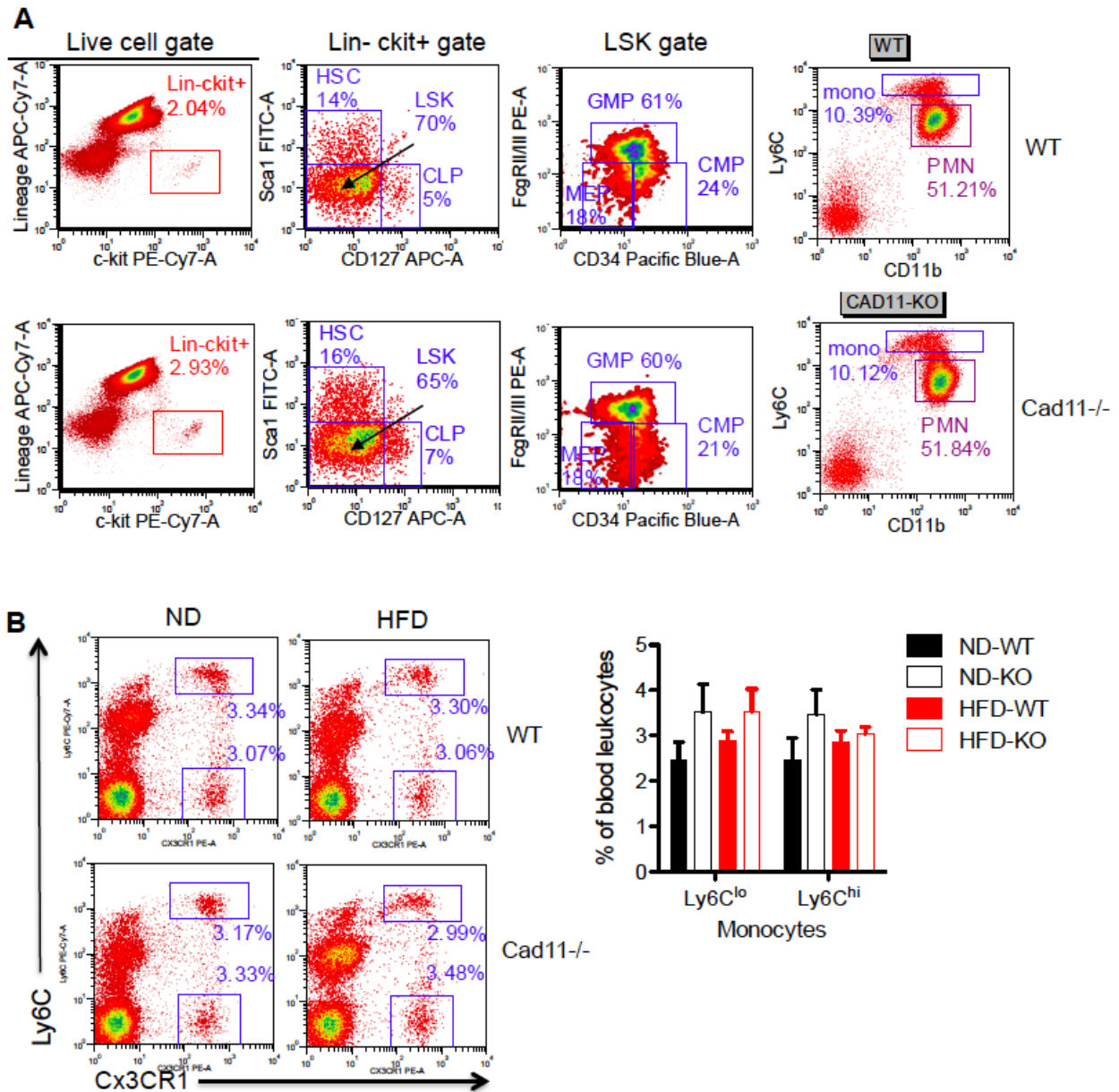
Supplemental Figure 1



Supplemental Figure 1

Flow cytometry gating strategy for cad-11 expression in CD45⁺ vs CD45⁻ of stromal vascular fraction cells.

Supplemental Figure 2

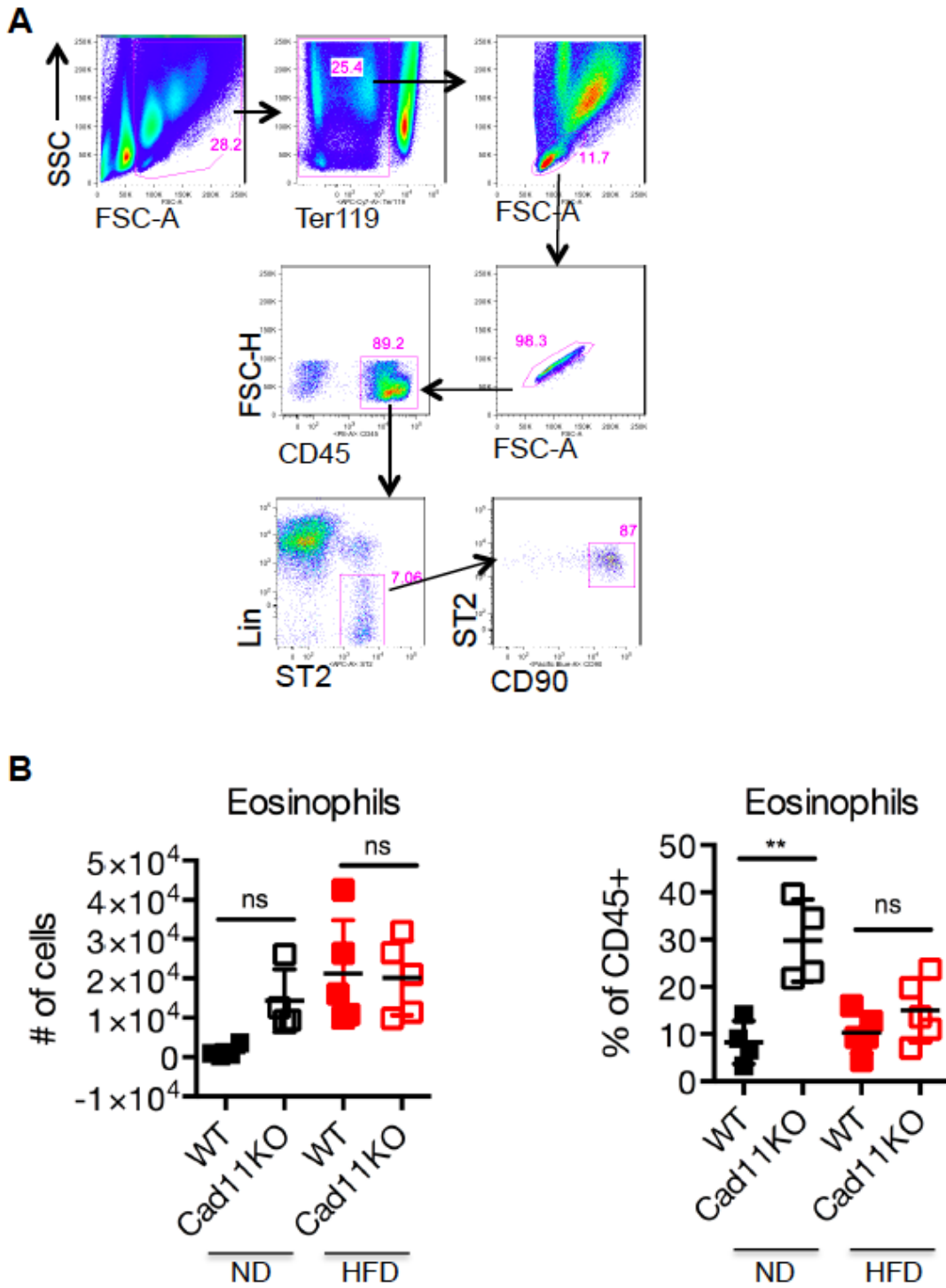


Supplemental Figure 2

Intact development of myeloid cell lineage in bone marrow of cad-11^{-/-} mice. (A) Flow cytometry plots and percentage of myeloid cell lineage development in bone marrow of lean WT and cad-11^{-/-} mice. HSC: hematopoietic stem cell (Lin⁻Sca1⁺ckit⁺), LSK: multipotent progenitors (Lin⁻Sca1⁻ckit⁺), CLP: common lymphoid progenitor (ckit⁺CD127⁺Sca1^{low}), CMP: common myeloid progenitor (ckit⁺CD127⁻CD34⁺FcgRII/III⁺), MEP: MK and erythrocyte progenitor (ckit⁺CD127⁻CD34⁻FcgRII/III⁻), GMP: granulocyte

macrophage progenitor ($\text{ckit}^+\text{CD127}^-\text{CD34}^{\text{lo}}\text{FcγRII/III}^{\text{hi}}$). **(B)** Flow cytometry plots (left panel) and percentage (right panel) of peripheral blood monocytes ($\text{Ly6C}^{\text{hi}}\text{CxCR3}^+$ or $\text{Ly6C}^{\text{lo}}\text{CxCR3}^+$) of lean and obese WT and $\text{cad-11}^{-/-}$ mice (n=4 ND-WT, n=4 ND-KO, n=5 HFD-WT, and n=5 HFD-KO).

Supplemental Figure 3

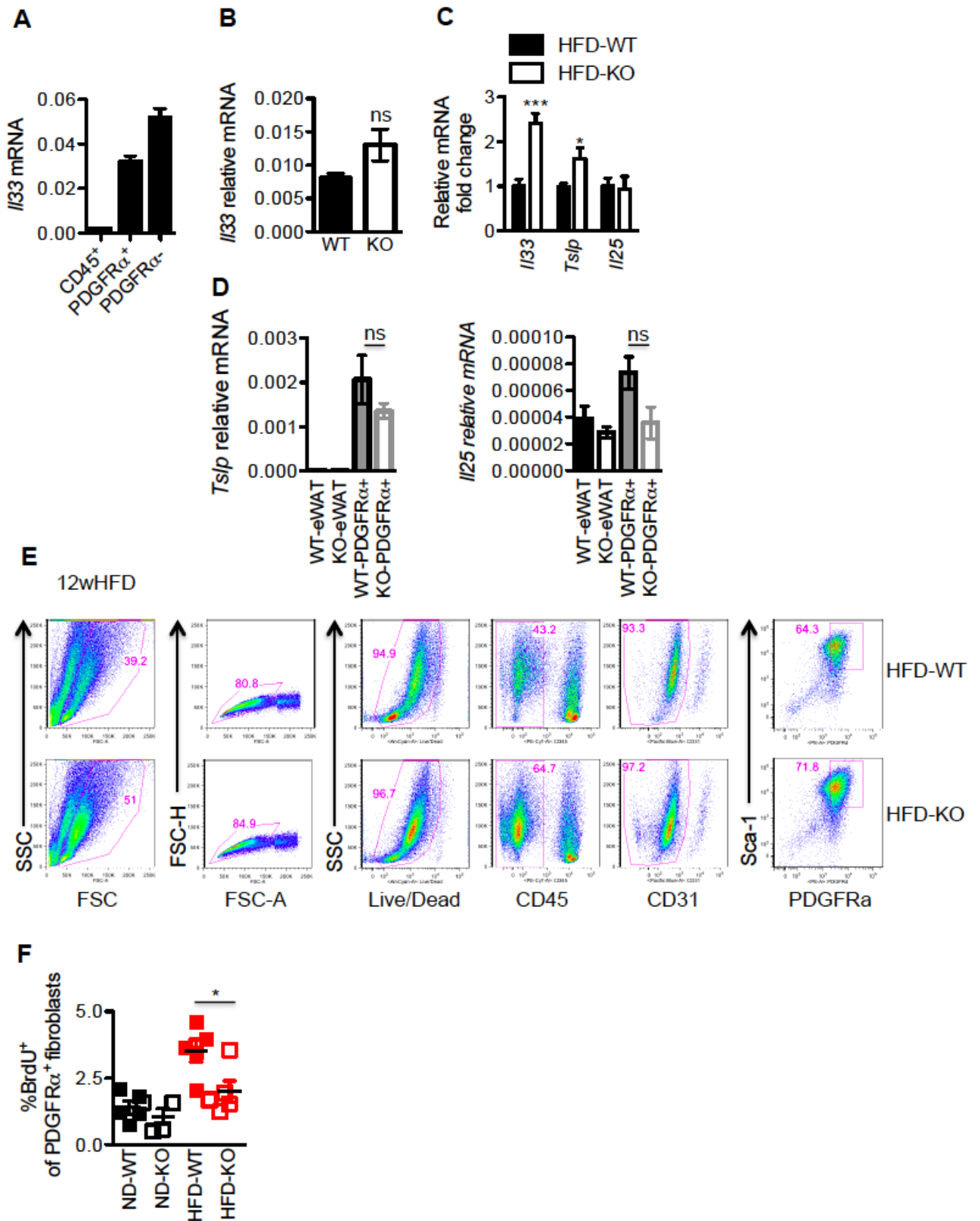


Supplemental Figure 3

(A) Flow cytometry gating strategy for ILC2 in stromal vascular fraction cells. (B) The number and percentage of eosinophils in adipose tissue of WT and *cad-11*^{-/-} mice fed a ND or HFD for 5 weeks (n=4 ND-WT, n=4 ND-KO, n=5 HFD-WT, and n=5 HFD-KO). **p<0.01, not

significant (n.s.). Data are expressed as mean \pm s.e.m. Statistical analysis was determined by Two-Way ANOVA test for B.

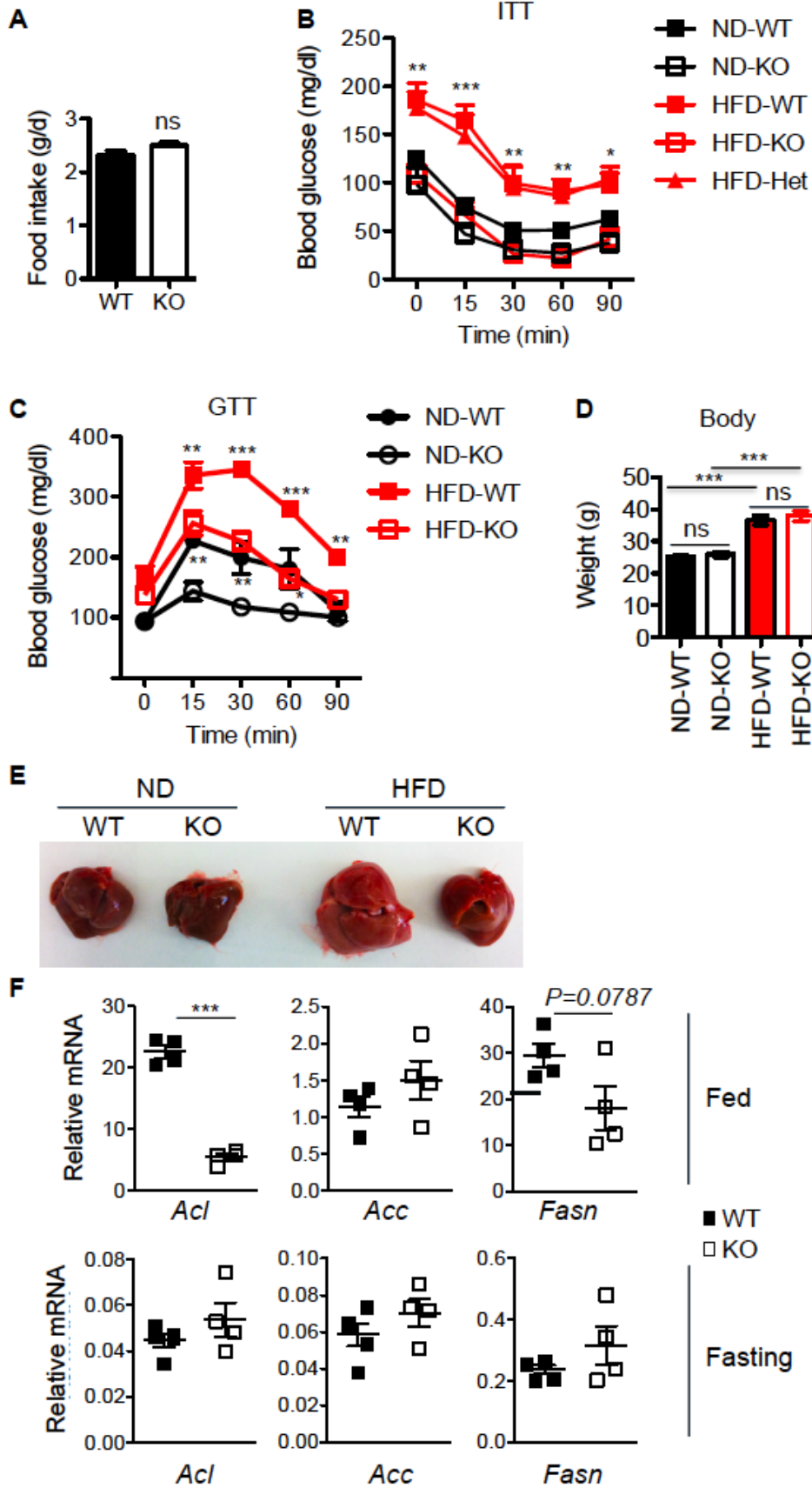
Supplemental Figure 4

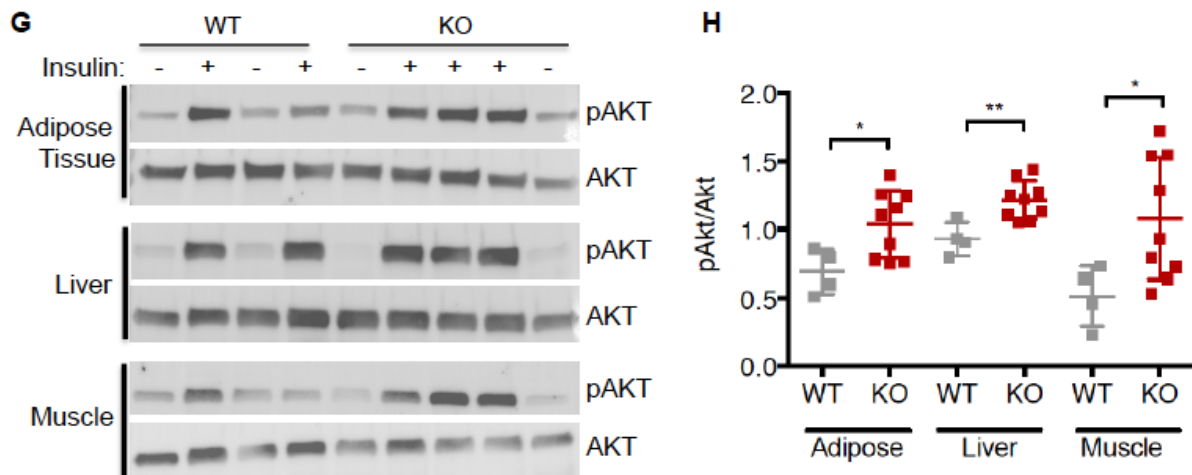


Supplemental Figure 4

IL-33 production by PDGFR α ⁺ fibroblasts. (A) IL-33 expression in sorted CD45⁺ cell, PDGFR α ⁺, and PDGFR α ⁻ cells from stromal vascular fraction cells in WT adipose tissue. (B) IL-33 expression in adipose tissue of lean WT and *cad-11*^{-/-} mice (n=5 ND-WT and n=5 ND-KO), representative of two independent experiments. (C) mRNA expression of IL-33, TSLP, and IL25 in adipose tissue of HFD-fed mice for 10 weeks (n=6 HFD-WT, n=5 HFD-KO), representative of three independent experiments. (D) *Tslp* and *Il15* in adipose tissue or flow-isolated PDGFR α ⁺ fibroblasts (n=5 WT-eWAT, n=5 KO-eWAT, n=5 WT-PDGFR α ⁺, and n=5 KO-PDGFR α ⁺). (E) Flow cytometry gating strategy for PDGFR α ⁺ fibroblasts in adipose tissue. (F) The percentage of BrdU⁺ of PDGFR α ⁺ fibroblasts in adipose tissue of HFD-fed mice for 5 weeks (n=5 ND-WT, n=4 ND-KO, n=5 HFD-WT, n=5 HFD-KO). *p<0.05, **p<0.01, ***p<0.001, not significant (n.s.). Data are expressed as mean \pm s.e.m. Statistical analysis was determined by Student's unpaired *t* test for A, B, C, D, and F.

Supplemental Figure 5



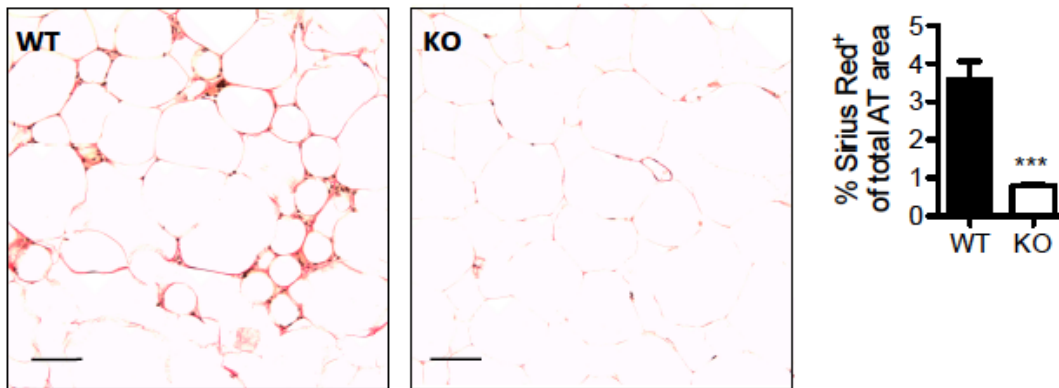


Supplemental Figure 5

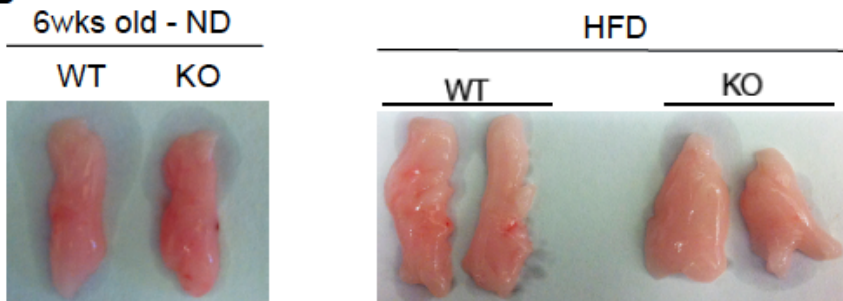
Cad-11^{-/-} mice are resistant to obesity-induced insulin resistance. (A) Daily food intake per mouse for the last two weeks of a 5-week HFD (n=5 WT, n=6 KO), representative of three independent experiments. (B) ITT were performed on WT and cad-11^{-/-} littermates fed a HFD for 5 weeks (n=5 ND-WT, n=3 ND-KO, n=7 HFD-WT, n=7 HFD-Het, and n=5 HFD-KO), a single experiment. (C and D) GTT and body weight of WT and cad-11^{-/-} mice fed a HFD for 10 weeks (n=4 ND-WT, n=4 ND-KO, n=6 HFD-WT, and n=6 HFD-KO). (E) Representative liver picture of WT and cad-11^{-/-} mice fed a HFD for 12 weeks. (F) qPCR for lipogenesis genes in liver from fed and fasted mice on a HFD for 5 weeks (n=4 HFD-WT and n=4 HFD-KO), representative of two independent experiments. For G and H, after feeding mice HFD for 12 weeks, WT and cad-11^{-/-} mice were fasted for 6 hrs. Adipose tissue, liver, and muscle were taken at 3 min post- injection of insulin (20U/kg) via the inferior vena cava. (G) 50ug of lysates were loaded and membrane were blotted for pAKT or AKT. (H) The ratio of pAKT to AKT in each organ was shown in graph. n=4 HFD-WT and n=9 HFD-KO. A single experiment. *p<0.05, **p<0.01, ***p<0.001, not significant (n.s.). Data are expressed as mean ± s.e.m. Statistical analysis was determined by Student's unpaired *t* test for A, D, and F, H, and Two-Way ANOVA test for HFD-WT vs HFD-KO in B and C.

Supplemental Figure 6

A



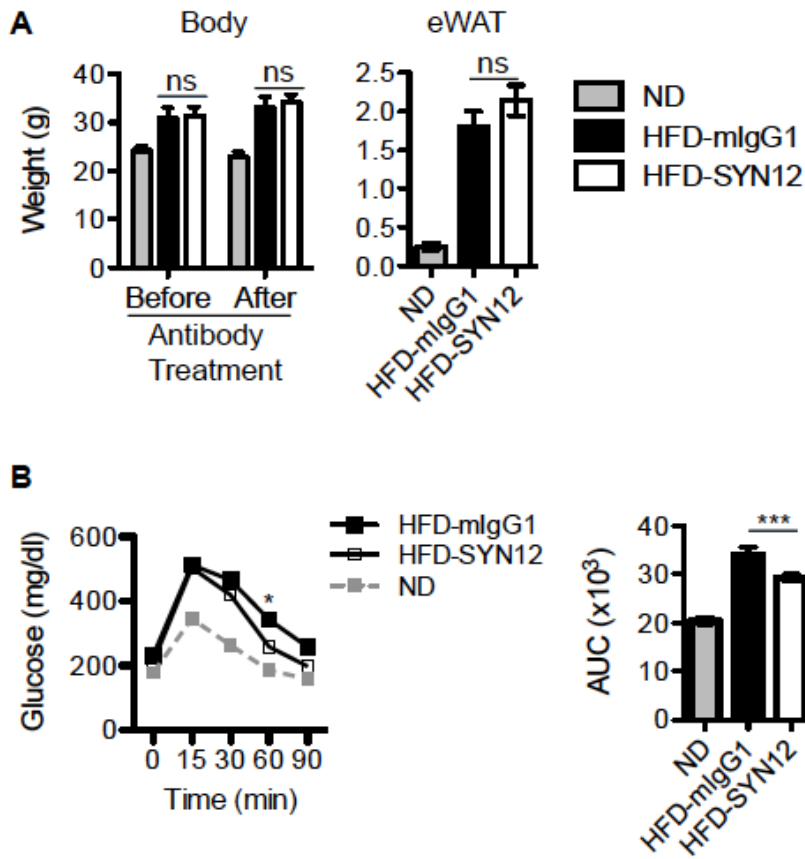
B



Supplemental Figure 6

Cad-11^{-/-} mice were protected from developing obesity-induced fibrosis. (A) WT and cad-11^{-/-} mice were fed a HFD for 12 weeks. Sirius Red staining in adipose tissue sections (left images) and the percentage positive for Sirius red staining of adipose tissue area (right graph) was measured by image J (n=5 HFD-WT and n=5 HFD-KO), representative of two independent experiments. Scale Bars, 100 μ m. **(B)** Representative fat pad picture of WT and cad-11^{-/-} lean and young (left) and obese (right) mice. *p<0.05, **p<0.01, ***p<0.001. Data are expressed as mean \pm s.e.m. Statistical analysis was determined by Student's unpaired *t* test for A.

Supplemental Figure 7



Supplemental Figure 7

Blockade of cad-11 improves glucose tolerance in obese WT mice. B6 WT mice were injected i.p. with anti-cad-11 specific antibody (SYN12) or mIgG1 isotype control antibody (500 μ g for the first injection and 100 μ g for the rest of injections) every three days for the last two weeks of a 5-week HFD (n=4 ND, n=5 HFD-mIgG1 and n=5 HFD-SYN12), representative of three independent experiments. **(A)** Body weight and fat pad weight. **(B)** GTT and AUC. *p<0.05, ***p<0.001, not significant (n.s.). Data are expressed as mean \pm s.e.m. Statistical analysis was determined by Student's unpaired *t* test for A and B, AUC graph and Two-Way ANOVA test for mIgG1-treated HFD vs SYN12-treated HFD in B, GTT graph.